

## Structure of Binary Liquid Mixtures. I\*

N. W. ASHCROFT AND DAVID C. LANGRETH

*Laboratory of Atomic and Solid State Physics, Cornell University, Ithaca, New York*

(Received 15 November 1966)

An exact solution of the Percus-Yevick equation for the correlation functions  $C_{ij}(r)$  appropriate to a binary mixture has been given by Lebowitz. We show that the Fourier transforms  $C_{ij}(K)$  lead directly to the structure factors  $S_{ij}(K)$ , the latter being functions of a total packing parameter  $\eta$ , the ratio of the hard-sphere diameters and the concentration parameter  $x$  describing the relative amount of each component in the mixture. An expression for the compressibility is also given. The results are applied to a discussion of x-ray scattering from mixtures.

### I. INTRODUCTION

IN a recent paper Ashcroft and Lekner<sup>1</sup> demonstrated that the structure factor  $S(K)$  for a real single-component liquid (in fact, a liquid metal) could be well represented in the region up to and including the principal diffraction peak by the solution<sup>2,3</sup> of the Percus-Yevick equation for a system of rigid non-attracting spheres. Further discussion on the apparent success of this elementary model has recently been given by Verlet.<sup>4</sup> In view of the over-all agreement obtained and the wide applicability of the Percus-Yevick (PY) equation, it is natural to attempt an extension to binary systems for which solutions for the three correlation functions are already known.<sup>5</sup> Defining  $g_{ij}(r)$  to be the radial distribution function for the two-component mixtures, the PY equation may be written [cf. Eq. (8) in Ref. 5]

$$g_{ij}(r)(e^{-\beta\phi_{ij}(r)} - 1) = e^{-\beta\phi_{ij}(r)} C_{ij}(r), \quad (1)$$

where the  $C_{ij}(r)$  are the direct correlation functions, and  $\phi_{ij}(r)$  are the pair potentials.

The solutions to (1) for the special case of hard-sphere interactions between the components has been given in detail by Lebowitz.<sup>5</sup> We repeat these briefly in Sec. II: We also derive the structure factors<sup>6</sup>  $S_{ij}(K)$  and proceed to their evaluation for a general packing fraction  $\eta$ , for arbitrary ratio of hard-sphere diameters  $\sigma_1$  and  $\sigma_2$  and for any relative concentration. In Sec. III, the results are applied to the evaluation of typical x-ray scattering factors for some selected mixtures. We also consider the effects of impurities on both the scattering factors and the compressibility.

\* Work supported by the Advanced Research Projects Agency through the Materials Science Center at Cornell University, Ithaca, New York.

<sup>1</sup> N. W. Ashcroft and J. Lekner, Phys. Rev. **145**, 83 (1966) to be referred to as I.

<sup>2</sup> M. Wertheim, Phys. Rev. Letters **8**, 321 (1963).

<sup>3</sup> E. Thiele, J. Chem. Phys. **38**, 1959 (1963).

<sup>4</sup> L. Verlet, Advan. Phys. (to be published).

<sup>5</sup> J. L. Lebowitz, Phys. Rev. **133**, A895 (1964).

<sup>6</sup> Solutions similar to those set out here have been used by Enderby, North, and Egelstaff [Phil. Mag. **14**, 961, (1966)] in their recent analysis of neutron scattering data from the Cu-Sn system.

### II. STRUCTURE FACTORS

We adopt the following definitions and conventions. First, we arbitrarily choose the component 2 of the mixture to possess the larger hard-sphere diameter  $\sigma_2$ . We define  $\alpha$  to be the hard-sphere ratio

$$\alpha = \sigma_1/\sigma_2, \quad (0 \leq \alpha \leq 1).$$

Second, if there are  $N_1$  hard spheres of diameter  $\sigma_1$  and  $N_2$  with diameter  $\sigma_2$  (in the volume  $V$ ), we define  $x$  to be the concentration of larger spheres, that is,

$$x = \frac{N_2}{N_1 + N_2} = \frac{n_2}{n_1 + n_2} = \frac{n_2}{n},$$

where the small  $n_i$ 's represent the respective number densities,  $n$  being the total number density. In the notation of I, we set  $\eta$  equal to the total packing fraction for the mixture:

$$\eta = \frac{\text{volume occupied by hard spheres}}{\text{total volume}} = \eta_1 + \eta_2,$$

where  $\eta_i = (\pi/6)n_i\sigma_i^3$ ,  $i = 1, 2$ . It follows that

$$\eta_1 = \left( \frac{(1-x)\alpha^3}{x + (1-x)\alpha^3} \right) \eta$$

and

$$\eta_2 = \left( \frac{x}{x + (1-x)\alpha^3} \right) \eta. \quad (2)$$

The variables  $\eta$ ,  $\alpha$ , and  $x$  completely specify the system, and the coefficients in the various correlation functions listed below can be expressed solely in terms of them. For the Fourier transforms we require a wave-number space variable: We choose  $y = K\sigma_2$ , all other  $K$ -space variables being scaled to this (e.g.,  $K\sigma_1 = \alpha y$ , etc.).

The solutions of Eq. (1) given by Lebowitz for the mixture of hard spheres are

$$\begin{aligned} -C_{11}(r) &= a_1 + b_1 r + d r^3, & r < \sigma_1 \\ -C_{22}(r) &= a_2 + b_2 r + d r^3, & r < \sigma_2 \\ -C_{12}(r) &= a_1, & r < \frac{1}{2}(\sigma_2 - \sigma_1) \\ &= a_1 + [bR^2 + 4dR^3 + dR^4]/r, & \frac{1}{2}(\sigma_2 - \sigma_1) < r < \frac{1}{2}(\sigma_2 + \sigma_1), \end{aligned} \quad (3)$$

where  $R=r-\frac{1}{2}(\sigma_2-\sigma_1)$ , and  $\lambda=\frac{1}{2}(\sigma_2+\sigma_1)$ . The coefficients  $a_i$ ,  $b_i$ ,  $b$ , and  $d$  are simple but lengthy functions of  $\eta$ ,  $\alpha$ , and  $x$ , and their definitions are relegated to Appendix A. From Eqs. (3), we can immediately write down the Fourier transforms  $-n_1C_{11}(y)$ ,  $-n_2C_{22}(y)$ , and  $(n_1n_2)^{1/2}C_{12}(y)$  required in the definition of the structure factors. The details are set out in Appendix B. If we define

$$\tilde{S}_{ij}=S_{ij}(y)-1, \quad (4)$$

where

$$S_{ij}(k)=(N_iN_j)^{-1/2}\langle\sum_{n,m}e^{ik\cdot(r_n^i-r_m^j)}\rangle-(N_iN_j)^{1/2}\delta_{k,0},$$

then the definition of the direct correlation function gives immediately

$$\begin{aligned} n_1^{-1}\tilde{S}_{11}(y) &= C_{11}(y) + \tilde{S}_{11}(y) \\ &\quad + n_2^{1/2}n_1^{-1/2}\tilde{S}_{12}(y)C_{12}(y), \\ n_1^{-1/2}n_2^{-1/2}\tilde{S}_{12}(y) &= C_{12}(y) + \tilde{S}_{11}(y)C_{12}(y) \\ &\quad + n_2^{1/2}n_1^{-1/2}\tilde{S}_{12}(y)C_{22}(y), \\ n_1^{-1/2}n_2^{-1/2}\tilde{S}_{12}(y) &= C_{12}(y) + n_1^{1/2}n_2^{-1/2}\tilde{S}_{12}(y)C_{11}(y) \\ &\quad + \tilde{S}_{22}(y)C_{12}(y), \\ n_2^{-1}\tilde{S}_{22}(y) &= C_{22}(y) + n_1^{1/2}n_2^{-1/2}\tilde{S}_{12}(y)C_{12}(y) \\ &\quad + \tilde{S}_{22}(y)C_{22}(y), \end{aligned} \quad (5)$$

since  $C_{21}=C_{12}$ .

By use of (4), the solutions for the structure factors  $S_{ij}(y)$  can be found from (6) and are

$$\begin{aligned} S_{11}(y) &= \{1 - n_1C_{11}(y) - n_1n_2C_{12}^2(y)/[1 - n_2C_{22}(y)]\}^{-1}, \\ S_{22}(y) &= \{1 - n_2C_{22}(y) - n_1n_2C_{12}^2(y)/[1 - n_1C_{11}(y)]\}^{-1}, \\ S_{12}(y) &= (n_1n_2)^{1/2}C_{12}(y)\{[1 - n_1C_{11}(y)] \\ &\quad \times [1 - n_2C_{22}(y)] - n_1n_2C_{12}^2(y)\}^{-1}, \end{aligned} \quad (6)$$

which may be compared with the corresponding expression for a single-component system

$$S(y) = \{1 - nC(y)\}^{-1}.$$

The quantities  $S_{ij}(0)$  are easily derived from the  $C_{ij}(0)$ , and application of the Ornstein-Zernike fluctuation argument gives the following expression for the isothermal compressibility<sup>7</sup>

$$nkT\chi_T = \frac{S_{11}(0)S_{22}(0) - S_{12}^2(0)}{(1-x)S_{22}(0) + xS_{11}(0) - 2[x(1-x)]^{1/2}S_{12}(0)}, \quad (7)$$

or in terms of the  $C_{ij}(0)$ ,

$$nkT\chi_T = \{1 - (1-x)^2nC_{11}(0) - x^2nC_{22}(0) - 2x(1-x)nC_{12}(0)\}^{-1}, \quad (8)$$

<sup>7</sup> This follows quickly from writing the  $S_{ij}(0)$  in terms of the fluctuations in the number of particles from the mean, i.e.,  $\langle(N_iN_j)^{1/2}S_{ij}(0)\rangle = \langle N_iN_j \rangle - \langle N_i \rangle \langle N_j \rangle$ . See, for example, F. J. Pearson and G. S. Rushbrooke, Proc. Roy. Soc. (Edinburgh) **A64**, 305 (1957), and J. G. Kirkwood and F. P. Buff, J. Chem. Phys. **19**, 774 (1951). We also point out that Eq. (8) follows directly from Lebowitz's equation (13) (Ref. 5).

where  $x$  is the concentration of the larger component. We note in passing that Eqs. (4)–(8) are quite general and independent of the PY and hard-sphere approximations.

In terms of the parameters  $\eta$ ,  $x$ , and  $\alpha$ , the isothermal compressibility may be written

$$nkT\chi_T = (1-\eta)^4\{(1+2\eta)^2 - \Delta\}^{-1}, \quad (9)$$

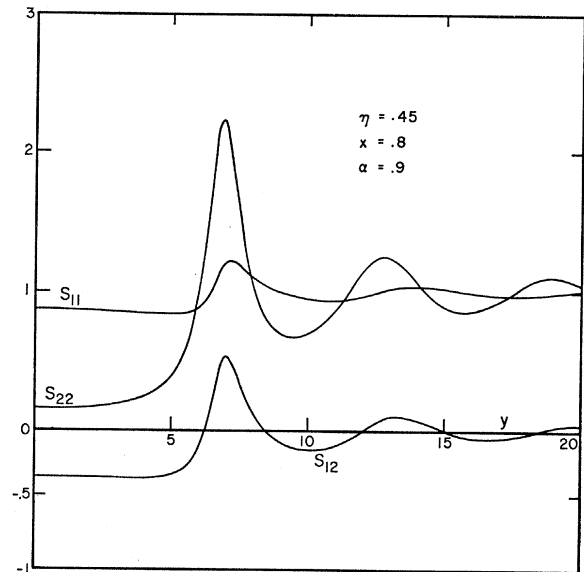


FIG. 1. Structure factors  $S_{ij}(y)$  for the combinations  $\eta=0.45$ ,  $\alpha=0.9$ , and  $x=0.8$ , where  $\eta$  is the total packing fraction,  $x$  the concentration of the larger species, and  $\alpha$  the ratio of hard-sphere diameters. The momentum-space variable  $y$  is the wave number times the larger hard-sphere diameter.

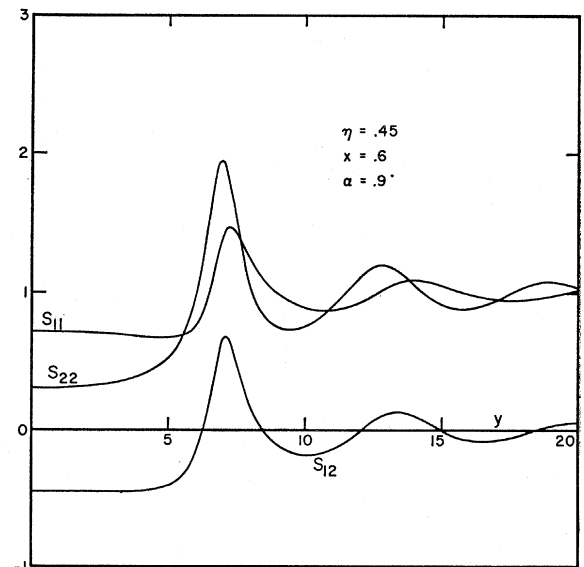


FIG. 2. Structure factors  $S_{ij}(y)$  for the combinations  $\eta=0.45$ ,  $\alpha=0.9$ , and  $x=0.6$ , where  $\eta$  is the total packing fraction,  $x$  the concentration of the larger species, and  $\alpha$  the ratio of hard-sphere diameters. The momentum-space variable  $y$  is the wave number times the larger hard-sphere diameter.

where

$$\Delta = \frac{3x(1-x)\eta(1-\alpha)^2}{x+(1-x)\alpha^3} \times \left\{ (2+\eta)(1+\alpha) + \frac{3\eta\alpha}{x+(1-x)\alpha^3} [(1-x)\alpha^2+x] \right\},$$

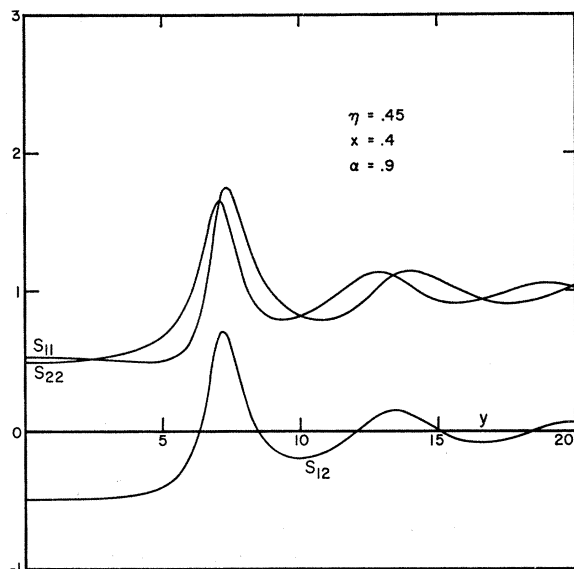


FIG. 3. Structure factors  $S_{ij}(y)$  for the combinations  $\eta=0.45$ ,  $\alpha=0.9$ , and  $x=0.4$ , where  $\eta$  is the total packing fraction,  $x$  the concentration of the larger species, and  $\alpha$  the ratio of hard-sphere diameters. The momentum-space variable  $y$  is the wave number times the larger hard-sphere diameter.

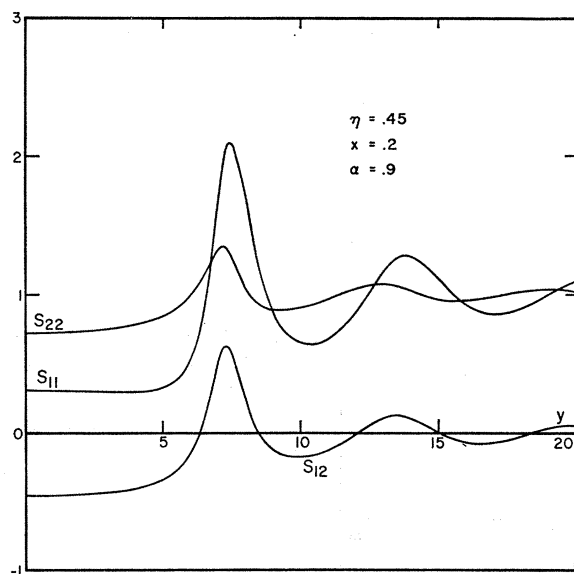


FIG. 4. Structure factors  $S_{ij}(y)$  for the combinations  $\eta=0.45$ ,  $\alpha=0.9$ , and  $x=0.2$ , where  $\eta$  is the total packing fraction,  $x$  the concentration of the larger species, and  $\alpha$  the ratio of hard-sphere diameters. The momentum-space variable  $y$  is the wave number times the larger hard-sphere diameter. Note in Figs. 1-4 the reversal in role of the behavior of the (11) and (22) structure factors as the concentration variable executes its full range.

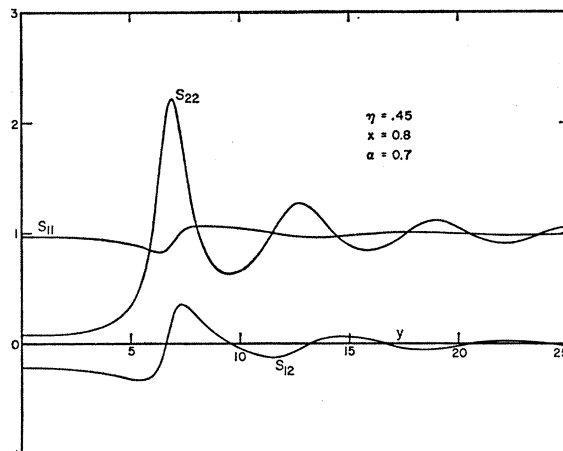


FIG. 5. Structure factors  $S_{ij}(y)$  for the combinations  $\eta=0.45$ ,  $\alpha=0.7$ , and  $x=0.8$ .

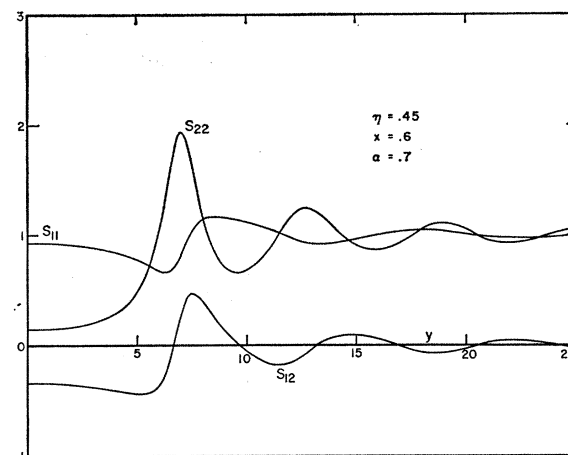


FIG. 6. Structure factors  $S_{ij}(y)$  for the combinations  $\eta=0.45$ ,  $\alpha=0.7$ , and  $x=0.6$ .

and for typical values of  $\eta \sim 0.45$ ,  $\alpha \gtrsim 0.6$ ,  $x \sim 0.7$ ,  $\Delta$  is usually considerably smaller than  $(1+2\eta)^2$ . For a pure single-component liquid,  $\Delta=0$ . In the limit  $\alpha \rightarrow 1$ , it is easy to see from Eqs. (3) and Appendices A and B that the three correlation functions  $C_{ij}(r)$  become identical. The sum

$$S = xS_{22}(y) + 2[x(1-x)]^{1/2}S_{12}(y) + (1-x)S_{11}(y)$$

is independent of the concentration  $x$ , as required, and reduces to

$$S = \{1 - nC(y)\}^{-1},$$

(which is also a general result).

### III. RESULTS AND DISCUSSION

It is a straightforward matter to compute the  $S_{ij}(y)$  for any combination of  $\eta$ ,  $\alpha$ , and  $x$ . For purposes of illustration we have chosen  $\eta=0.45$ , the value of the packing fraction close to that observed in the classical

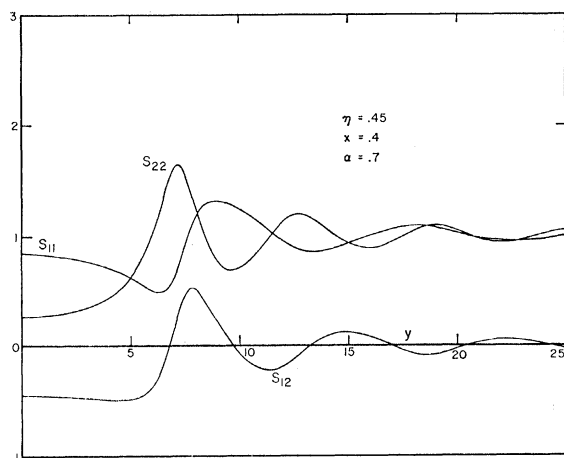


FIG. 7. Structure factors  $S_{ij}(y)$  for the combinations  $\eta=0.45$ ,  $\alpha=0.7$ , and  $x=0.4$ .

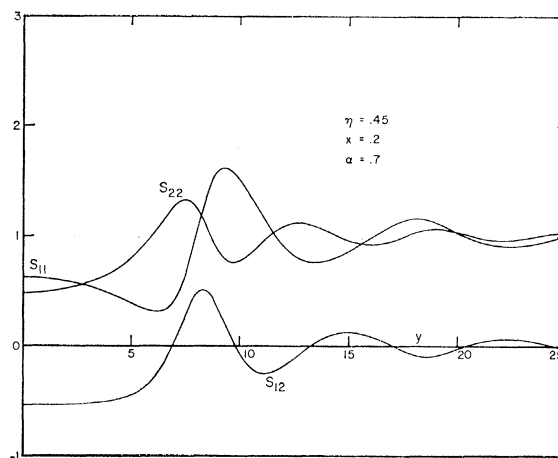


FIG. 8. Structure factors  $S_{ij}(y)$  for the combinations  $\eta=0.45$ ,  $\alpha=0.7$ , and  $x=0.2$ .

hard-sphere phase transition<sup>8</sup> in a pure liquid. We expect that as for single-component liquids, physically interesting values of  $\eta$  will occur in the neighborhood of  $\eta=0.45$ .

The curves of Figs. 1-8 show the three structure factors  $S_{11}(y)$ ,  $S_{22}(y)$ , and  $S_{12}(y)$  and the hard-sphere ratio and concentration are given the values indicated on the diagrams. For low values of concentration (of the larger species) we find as expected that  $S_{22}(y) \sim 1$ , while  $S_{11}(y)$  has the general features of  $S(y)$  for a pure liquid. At the same low concentration, however, the cross-structure factor departs appreciably from zero, especially at low  $y$ . An interesting aspect of the curves is the positioning of the principal peaks. For moderate

concentrations, they seem to bear no simple numerical relationship to the hard-sphere ratio as might have been anticipated. It is apparent, however, that the peak of  $S_{22}(y)$  lies closer to  $y=0$  than the peak of  $S_{11}(y)$ , with the peak of  $S_{12}(y)$  occurring midway between them. When the hard-sphere diameters are considerably different ( $\alpha \lesssim 0.5$ ) the modifications to the structure factor for the majority component are particularly severe. We find that the important parameter in gauging the effectiveness of the large component is, of course,  $\alpha^{-3}x$ . Figures 9-12 show  $S_{ij}(y)$  for low concentrations of a large second component ( $\alpha=0.5$ ). We have used curves of this kind to evaluate the effect of small amounts of a second component in the x-ray scattered

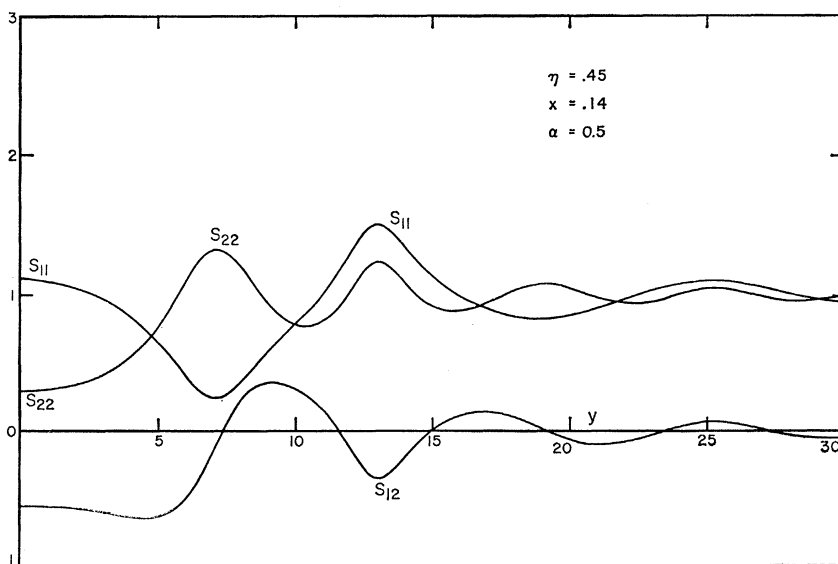
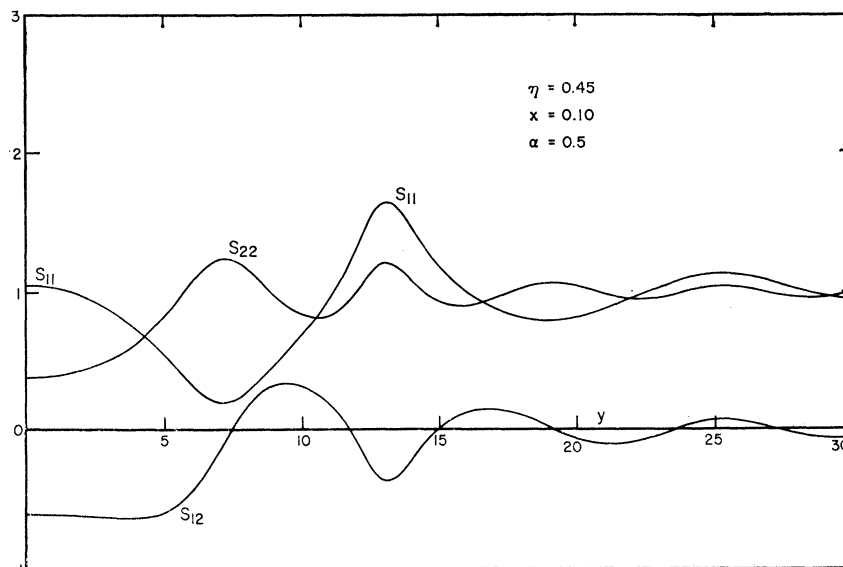


FIG. 9. Structure factors  $S_{ij}(y)$  for low concentrations of a second component whose diameter is twice that of the host. Again  $\eta=0.45$  and the concentration parameter  $x=0.14$ .

<sup>8</sup> T. Wainwright and B. Alder, *Nuovo Cimento Suppl.* **9**, 116 (1958).

FIG. 10. Structure factors  $S_{ij}(y)$  for low concentrations of a second component whose diameter is twice that of the host. Again  $\eta=0.45$  and the concentration parameter  $x=0.10$ .



intensities from liquids. To obtain the intensity we require

$$I \propto x S_{22}(y) f_2^2(y) + 2[x(1-x)]^{1/2} S_{12}(y) f_1(y) f_2(y) + (1-x) S_{11}(y) f_1^2(y), \quad (10)$$

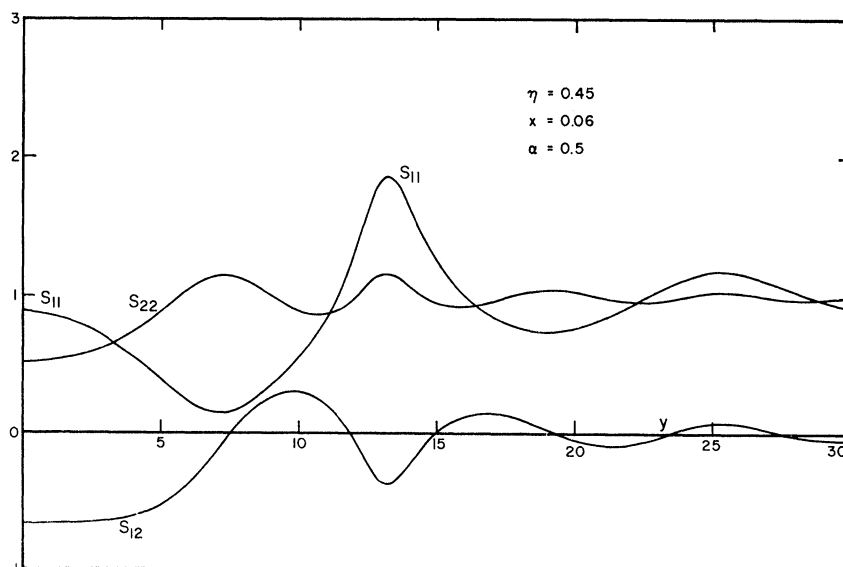
where  $f_i(y)$  are the atomic scattering factors appropriate to the two components. As the changes in the liquid structure are pronounced at low  $y$ , it is sufficient to demonstrate the effects by using the long-wavelength form of the scattering functions  $f_i(y)$ . We have taken the  $f_i(y)$  to be equal to the Fourier transform of a uniform distribution of total charge  $Z_i$  spread over a radius chosen to give approximately the correct long-wavelength variation. It is apparent from Figs. 13 and 14 that even small concentrations of a second

component can appreciably distort the structure factor of the pure-host liquid. The major effect occurs at small  $y$ , although there is a noticeable shift in the height of the principal diffraction peak.

#### IV. CONCLUSION

We have shown that the three structure factors of a binary mixture derived from the solution of the PY equation can be expressed in closed form in terms of simple functions. For a given mixture, the  $S_{ij}(y)$  are controlled by the three parameters  $\eta$ ,  $x$ , and  $\alpha$ . It is a straightforward matter to evaluate quantities depending on various weights of the  $S_{ij}(y)$ , and we have given by way of example the intensity function for x-ray scattering. From the formulas given in Appendices A and B

FIG. 11. Structure factors  $S_{ij}(y)$  for low concentrations of a second component whose diameter is twice that of the host. Again  $\eta=0.45$  and the concentration parameter  $x=0.06$ .



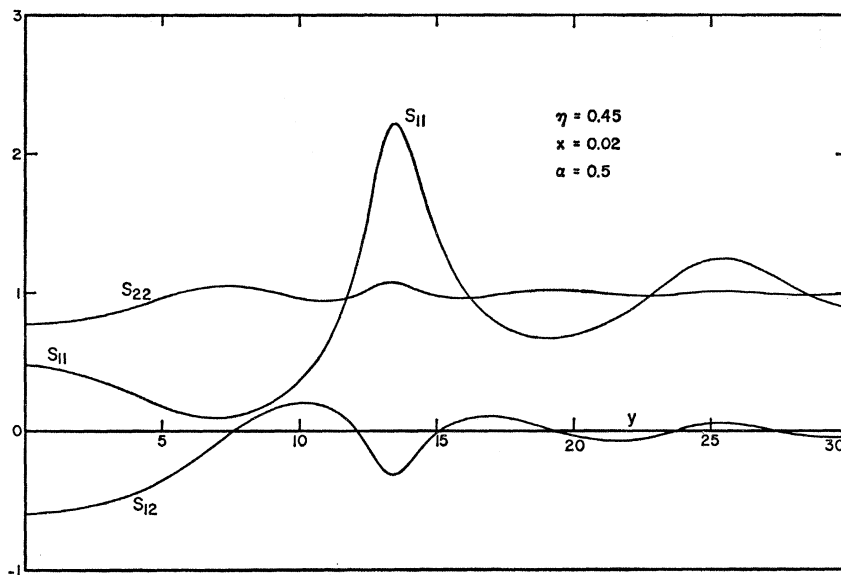


FIG. 12. Structure factors  $S_{ij}(y)$  for low concentrations of a second component whose diameter is twice that of the host. Again  $\eta=0.45$  and the concentration parameter  $x=0.02$ . Note that even at the lowest concentration (2%) the additional component has a pronounced effect.

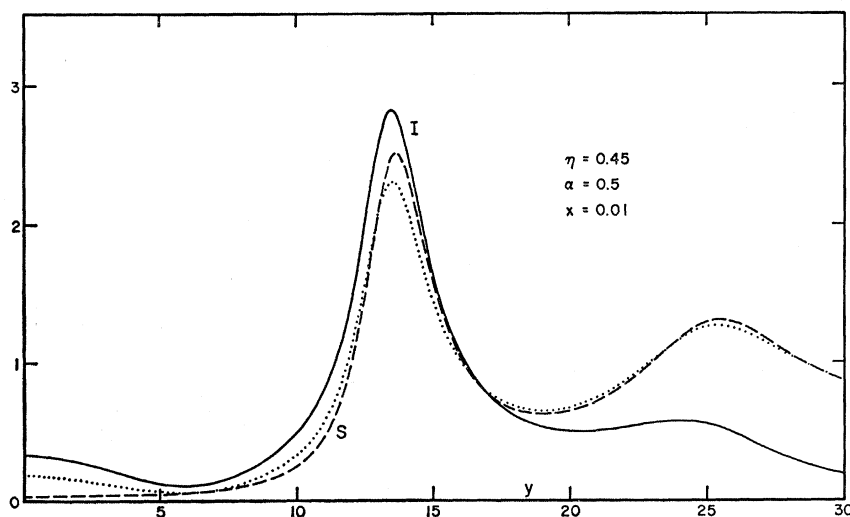


FIG. 13. The dashed curve is the structure for a pure single-component system with packing fraction  $\eta=0.45$ . The full curve  $I$  is the intensity (in arbitrary units) calculated according to Eq. (10) using  $Z_2=88$ ,  $Z_1=80$ ,  $\alpha=0.5$ , and  $x=0.01$ . The dotted curve is obtained from  $I$  by assuming it to be a pure liquid and simply dividing by the atomic scattering factor appropriate to  $Z_1$ . The result, compared with  $S$ , is thereby an indication of the discrepancy expected when an assumed pure sample of liquid Hg has an impurity level of 1% of HgO (which we take to be twice as large as Hg).

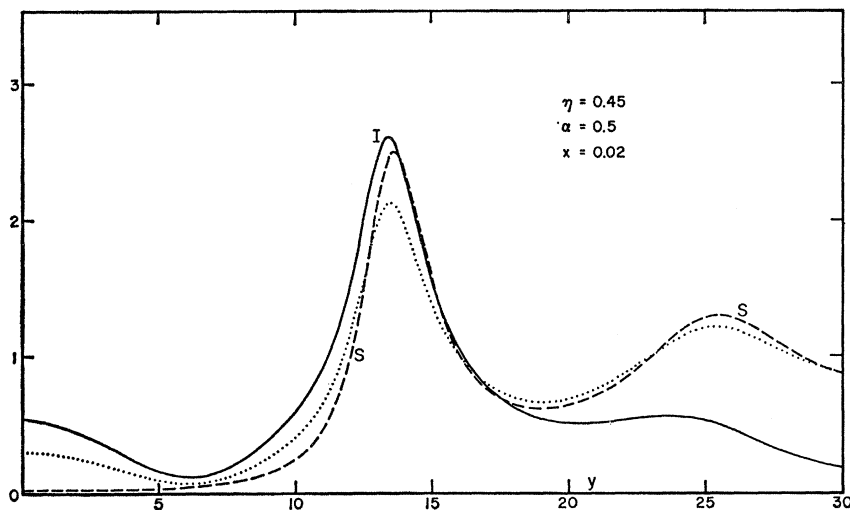


FIG. 14. The dashed curve is the structure for a pure single-component system with packing fraction  $\eta=0.45$ . The full curve  $I$  is the intensity (in arbitrary units) calculated according to Eq. (10) using  $Z_2=88$ ,  $Z_1=80$ ,  $\alpha=0.5$ , and  $x=0.02$ . The dotted curve is obtained from  $I$  by assuming it to be a pure liquid and simply dividing by the atomic scattering factor appropriate to  $Z_1$ . The result, compared with  $S$ , is thereby an indication of the discrepancy expected when an assumed pure sample of liquid Hg has an impurity level of 2% of HgO (which we take to be twice as large as Hg). It is apparent that the presence of a second component in an otherwise pure system causes a rise in the intensity at low-momentum transfers.

and from Eq. (10), it is clear that the intensity for x-ray (or neutron scattering) from mixtures is easily derived from the knowledge of  $\eta$ ,  $x$ , and  $\alpha$ . A further application is in the field of transport properties of binary liquid alloys which we hope to present shortly.

Finally, the detailed application of these results is hampered by the paucity of empirical information on the values of  $\eta$  and  $\alpha$  appropriate to real binary liquids. As already mentioned, pure liquids ( $\alpha=1$ ) just above their melting points exhibit packing fractions  $\eta$  close to 0.45. This is the value of  $\eta$  at which the hard-sphere phase transition is observed in the molecular dynamics calculations of Wainright and Alder.<sup>8</sup> It would, therefore, be of great interest to determine the packing fraction at which the analogous liquid-solid transition occurs in binary hard-sphere mixtures. Further, Eq. (9) with  $\alpha=0$  gives accurate values of  $\chi_T$  for the pure-liquid alkali metals. The knowledge of compressibility data in binary liquids combined with information on the hard-sphere transition in the mixture would determine both  $\eta$  and  $\alpha$  unambiguously. These data would lead to definitive predictions for both x-ray and neutron scattering intensities, which would presumably be accurate for momentum transfers up to and including the principal diffraction peaks.

#### ACKNOWLEDGMENTS

We are grateful for useful discussions with Dr. J. Enderby, and wish particularly to thank W. Francis for considerable assistance with the numerical computations.

#### APPENDIX A: THE CORRELATION FUNCTIONS $C_{ij}(r)$

The coefficient  $a_i$ ,  $b_i$ , etc. [Eq. (3)] given by Lebowitz<sup>5</sup> may be written as follows:

$$-n_1 C_{11}(y) = -\frac{24\eta_1}{\alpha^3 y^3} \left\{ a_1 (\sin \alpha y - \alpha y \cos \alpha y) + \frac{\beta_1}{\alpha y} [2\alpha y \sin \alpha y - (\alpha^2 y^2 - 2) \cos \alpha y - 2] \right. \\ \left. + \frac{\gamma_1}{\alpha^3 y^3} [(4\alpha^3 y^3 - 24\alpha y) \sin \alpha y - (\alpha^4 y^4 - 12\alpha^2 y^2 + 24) \cos \alpha y + 24] \right\}. \quad (\text{B1})$$

To obtain  $-n_2 C_{22}(y)$ , we simply replace  $\eta_1$  by  $\eta_2$ ,  $\alpha y$  by  $y$ ,  $\beta_1$  by  $\beta_2$ , and  $\gamma_1$  by  $\alpha^{-3}\gamma_1$ . The Fourier transform of  $C_{12}(r)$  is more complicated and is written

$$-n_1^{1/2} n_2^{1/2} C_{12}(y) = 3(1-\alpha)^3 \frac{\eta x^{1/2} (1-x)^{1/2}}{x+(1-x)\alpha^3} a_1 \frac{\sin y_\lambda - y_\lambda \cos y_\lambda}{y_\lambda^3} + 24\eta \frac{x^{1/2} (1-x)^{1/2} \alpha^3 \sin y_\lambda}{x+(1-x)\alpha^3} \left\{ \frac{\beta_{12}}{y_1^4} [2y_1 \cos y_1 + (y_1^2 - 2) \sin y_1] \right. \\ \left. + \frac{\gamma_{12}}{y_1} [(3y_1^2 - 6) \cos y_1 + (y_1^3 - 6y_1) \sin y_1 + 6] + \frac{\gamma_1}{y_1^2} [(4y_1^3 - 24y_1) \cos y_1 + (y_1^4 - 12y_1^2 + 24) \sin y_1] \right\} \\ \left. + \frac{\cos y_\lambda}{y_1^4} \left\{ \beta_{12} [2y_1 \sin y_1 - (y_1^2 - 2) \cos y_1 - 2] + \frac{\gamma_{12}}{y_1} [(3y_1^2 - 6) \sin y_1 - (y_1^3 - 6y_1) \cos y_1] \right. \right. \\ \left. \left. + \frac{\gamma_1}{y_1^2} [(4y_1^3 - 4y_1) \sin y_1 - (y_1^4 - 12y_1^2 + 24) \cos y_1 + 24] \right\} \right. \\ \left. + \frac{a_1}{y_1} \left\{ \cos y_\lambda \left( \frac{\sin y_1 - y_1 \cos y_1}{y_1^2} + \frac{1-\alpha}{2\alpha} \frac{1 - \cos y_1}{y_1} \right) + \sin y_\lambda \left( \frac{\cos y_1 + y_1 \sin y_1 - 1}{y_1^2} + \frac{1-\alpha}{2\alpha} \frac{\sin y_1}{y_1} \right) \right\} \right\}.$$

$$a_1 = \frac{\partial}{\partial \eta_1} (\beta \rho'),$$

$$a_2 = \alpha^{-3} \frac{\partial}{\partial \eta_2} (\beta \rho'), \quad (\text{A1})$$

where  $(\beta \rho')$  is the reduced function

$$(\beta \rho') = \{ (\eta_1 + \alpha^3 \eta_2) (1 + \eta + \eta^2) - 3\eta_1 \eta_2 (1 - \alpha)^2 \\ \times [1 + \eta_1 + \alpha(1 + \eta_2)] \} (1 - \eta)^{-3}.$$

In terms of the functions

$$g_{11} = \left[ \left(1 + \frac{1}{2}\eta\right) + \frac{3}{2}\eta_2(\alpha - 1) \right] (1 - \eta)^{-2},$$

$$g_{22} = \left[ \left(1 + \frac{1}{2}\eta\right) + \frac{3}{2}\eta_1 \left(\frac{1}{\alpha} - 1\right) \right] (1 - \eta)^{-2},$$

and

$$g_{12} = \left[ \left(1 + \frac{1}{2}\eta\right) + \frac{3}{2} \frac{1 - \alpha}{1 + \alpha} (\eta_1 - \eta_2) \right] (1 - \eta)^{-2},$$

we find

$$\beta_1 = \sigma_1 b_1 = -6 \left[ \eta_1 g_{11}^2 + \frac{1}{4} \eta_2 (1 + \alpha)^2 \alpha g_{12}^2 \right], \quad (\text{A2})$$

$$\beta_2 = \sigma_2 b_2 = -6 \left[ \eta_2 g_{22}^2 + \frac{1}{4} \eta_1 \alpha^{-3} (1 + \alpha)^2 g_{12}^2 \right], \quad (\text{A3})$$

$$\sigma_2 b = -3(1 + \alpha) \left[ \alpha^{-2} \eta_1 g_{11} + \eta_2 g_{22} \right] g_{12}, \quad (\text{A4})$$

and finally

$$\gamma_1 = \sigma_1^3 d = [\eta_1 a_1 + \alpha^3 \eta_2 a_2], \quad (\text{A5})$$

where the  $a_i$  are given above.

#### APPENDIX B: THE FOURIER TRANSFORMS $C_{ij}(y)$

Writing  $y_1 = K\sigma_1 = \alpha y$ , we find from (3)

Here we require the additional definitions

$$\gamma_\lambda = K\lambda = \frac{1}{2}y(1-\alpha),$$

$$\gamma_{12} = 4\lambda d\sigma_1^2 = 2\gamma_1 \left( \frac{1-\alpha}{\alpha} \right),$$

and

$$\beta_{12} = \sigma_1 b = -3\alpha(1-\alpha)(\alpha^{-2}\eta_{12}g_{11} + \eta_{22}g_{12}).$$

PHYSICAL REVIEW

VOLUME 156, NUMBER 3

15 APRIL 1967

## Resonance Scattering and the Electrical and Thermal Resistivities Associated with Extended Defects in Crystals

R. A. BROWN\*

*School of Mathematics and Physics, Macquarie University, New South Wales, Australia*

(Received 13 October 1966)

The general failure of theory to account for the observed electrical and thermal resistivities associated with dislocations is reviewed in the light of the resonance scattering previously shown to be a characteristic property of linear defects in crystals. Expressions for the scattering width and density of states near a resonance are obtained, and the magnitude of the resonance scattering is shown to be consistent with the observed electrical resistivity of dislocations in a number of metals. Observed stacking-fault electrical resistivities are consistent with the absence of resonance scattering; such scattering is not expected to occur for plane defects. The resonance-scattering mechanism is shown to be capable of accounting for the magnitude of the dislocation thermal resistivity in ionic crystals, and also, possibly, for the much smaller effect in metals. The observed temperature dependence of the thermal resistivity in ionic crystals is rather difficult to explain in terms of resonance scattering, although it would probably be expecting too much for the simple treatment given here to deal adequately with this point. The generally encouraging results would appear to justify the expenditure of more effort, both experimentally and theoretically, on these problems.

### I. INTRODUCTION

**R**ESONANCE scattering of electrons and phonons has been shown<sup>1</sup> to be a characteristic property of linear defects in crystals. In this paper, we attempt to investigate the role of these phenomena in determining the electrical and thermal resistivities associated with dislocations.

Previous theories have severely underestimated these resistivities, and the situation is briefly reviewed in Sec. II; the existence of resonance scattering opens all these theories to a rather more definite criticism than appears to have been previously leveled, and we may feel reasonably confident in suggesting that this mechanism provides a basic reason for the failure of the theory to date.

The remainder of this paper is devoted to the more positive procedure of showing how resonance scattering fits in with the currently available experimental data on the electrical and thermal resistivities associated with line and plane defects. Thus, in Sec. III, we develop simple expressions for the resistivities, in a form convenient for such an analysis, and in Sec. IV develop expressions for the dislocation scattering width near a

resonance, and in particular obtain the phase shifts to be used in the resistivity formulas of Sec. III. The density of states near a resonance is considered in Sec. IV B. The relation of the experimental data to the existence of resonance scattering is discussed in Sec. V.

Analysis of the electrical-resistivity data is particularly encouraging in that resonance scattering is indicated to occur, for the two types of defect, in just the way predicted by the theory<sup>1</sup>; that is to say, it appears to be both necessary and sufficient to explain the data on dislocations, at least for those cases where these data appear most reliable, but is not necessary to explain stacking-fault resistivities. The need for more accurate experimental work on a greater number of metals is evident, and it is hoped that the results of the present analysis are sufficiently promising to encourage such measurements.

The situation with the dislocation thermal resistivity is not quite so happy. On the one hand, the *magnitude* of the observed resistivity in the alkali halides is such as to be consistent with resonance scattering, and also the apparent absence of resonances in the low-temperature phonon scattering from metals<sup>2</sup> is not an insurmountable difficulty, at least at the present shallow level of investigation. On the other hand, it seems impossible,

\* Present address: School of Mathematics and Physics, Macquarie University, New South Wales, Australia.

<sup>1</sup> R. A. Brown, *Phys. Rev.* **156**, 889 (1967).

<sup>2</sup> See Ref. 27, however.